International Journal of Civil Engineering (IJCE)
ISSN(P): 2278-9987; ISSN(E): 2278-9995
Vol. 3, Issue 3, May 2014, 155-166

International Academy of Science, Engineering and Technology
Connecting Researchers; Nurturing Innovations

ANALYSIS OF BUCKLING LOAD FOR MICROPILES EMBEDDED IN A WEAK SOIL UNDER VERTICAL AXIAL LOADS

ALNOS ALY E. HEGAZY

Associate Professor, Department of Civil Engineering, Benha Faculty of Engineering, Benha University, Qalyubia, Egypt

ABSTRACT

A theoretical approach for buckling of micropiles fully embedded in a weak soil is presented in this study using nonlinear equations. A method has been developed to predict relationships between the critical buckling load and the lateral deflection for a single micropile subjected to vertical axial load. Nonlinearity of soil was considered using subgrade reaction. Therefore, the buckling of the micropile was formulated by using the small-angle bending theory. The governing nonlinear equations for the buckling of micropiles depend on the exact expressions of the curvatures and the finite-difference method which were used to formulate the mathematical model. The controlling factors such as subgrade reaction coefficients, boundary conditions and pile dimensions were considered in the analysis, applications and calculations. Comparisons between the results of the present analysis and those obtained from the p-y analysis show a good agreement. Also, comparisons show the accuracy of the present analysis. Additionally, the results indicated that the present analysis and is rational and easy for application and using.

KEYWORDS: Buckling, Finite-Differences, Lateral Deflection, Micropiles, Numerical Analysis, Numerical Application, Weak Soil

INTRODUCTION

Micropiles are slender elements and defined as small diameter piles, less than 300 mm and normally between 100-250 mm. They mainly transfer their loads by skin friction because the surface area of micropile is typically hundreds times larger than the base area. Therefore, the ultimate load which can be supported by a single micropile is defined by: (1) structural shaft resistance, (2) buckling load, or (3) failure of the grout/soil bond. However, the allowable load of micropile may be specified due to limitations of stresses and/or settlements that can be accepted by the structure being underpinned [1-4].

During last years, micropiles have been widely used in strengthening archaeological, historical and new buildings [5]. So, theoretical analysis, numerical applications and experimental works are necessary and required to understand the behavior of micropiles. Moreover, the analysis of micropile buckling is strongly required if the micropiles are installed through weak soil. Many researchers such as Abou-Rayan [6] and Ashour and Norris [7] have considered a simplified approach for the analysis of single traditional pile under direct lateral loads.

Their analysis was based on the variation approach along with the finite element method. Where, the flexural bending of the pile is modeled by linear-elastic beam elements. In their investigations, the applied load was considered as direct lateral forces at the free top on the pile upper end. Moreover, Zanuy et al. [8] mentioned that no enough attention was given to the lateral force effect as a consequence of micropile vertical axial load.

There are many problems concerning the design and the methodology of using micropiles as: (1) cavities are filled with fines or empty, (2) partially or fully embedded micropiles in a very weak soil, (3) the manner of applied load, (4) buckling may be occur, (5) difficulties of constructions, ...etc. When a portion of the micropile has to be exposed by an excavation, buckling should be considered and piles may need to be connected horizontally [9,10,11,12]. Similar to the analysis of columns, the free standing part of micropiles suffers from high compressive forces without any lateral resistance. Thus, the use of large-angle bending theory in the analysis is required to investigate the post-buckling behavior for slender elements. So, the surrounding soil provides lateral supports for the embedded part of micropiles. Therefore, buckling is somewhat limited in the embedded zone. Hence, the use of small-angle bending theory (classical bending theory) is sufficient for the analysis [6,7,10,11].

The influence of axial deformation is taken into account to simulate the micropile behavior correctly. Therefore, the micropile is considered to buckle as one unit. Hence, the embedded and free standing parts of micropile are assembled together to estimate the buckling load. The complexity of the problem requires a considerable number of iterations to obtain the suitable solution, [8,13,14]. Therefore, this study provides a theoretical analysis for the critical buckling load of a micropile embedded in a weak soil using the finite-difference approach. The considered parameters as: (a) the surrounding soil subgrade reaction modulus, (b) boundary conditions at lower and upper end of micropile, and (c) Micropile dimensions (pile length) are varied. So, for each of the variables an entire family of solutions is desirable to effectuate an optimum design.

THEORETICAL ANALYSIS

The analysis is conducted on an elastic micropile of length (L), constant cross sectional area (A), moment of inertia (I) and modulus of elasticity (E) subjected to an axial load not exceeding the micropile critical load (Q_{cr}). The pile is fully embedded in a soft soil. The necessary and required assumptions for the theoretical analysis are: (a) the pile is considered completely straight, elastic and subjected to vertical variant forces (Q) along its vertical axis, (b) the geometric properties of the cross section and material are constant along the micropile length, and (c) the pile deformations are small and enough to use the linear small-angle bending theory. Additionally, the micropile is modeled as a continuous elastic linear beam on a Winkler foundation having: (1) lateral or normal modulus of subgrade reaction (K_a), (2) tangential modulus of subgrade reaction (K_t), and (3) subgrade reaction modulus of soil under the pile base (K_b).

These reactions are represented by elastic linear springs as shown in Figure 1. Also, in this figure, v is the axial shortening in the pile at x-coordinate and f is the lateral deflection in the pile at y-coordinate. For the theoretical analysis, a small element (C-D) of length $dx=dL$ is studied. The forces and moments on the element C-D are shown and indicated in Figure 2. Hence, the vertical and lateral directions equilibrium of C-D element is analyzed and applied the following:

Vertical Direction Equations

From the equilibrium of forces in the vertical direction, as shown in Figure 2, the following equation can be written as:

$$\frac{dQ}{dx} - K_t.v = o \tag{1}$$

According to the linear stress-strain relationship, the applied axial load can be expressed in the following equation:

$$Q = E.A.\frac{dv}{dx} \tag{2}$$

By differentiating Q with respect to x at equation (2), the following equation is obtained as:

$$\frac{dQ}{dx} = E.A.\frac{d^2v}{dx^2} \tag{3}$$

Then, by using the obtained data in equation (3), the equation (1) becomes:

$$E.A.\frac{d^2v}{dx^2} - K_t.v = 0 \tag{4}$$

Referring to equation (4), it is evident that, equation (4) is the governing linear differential equation (second-order) for the axial deflection $v=v(x)$. Therefore, the logical boundary condition at the pile base (i.e. at x = 0.0) is:

$$\left(E.A.\frac{dv}{dx}\right)_{x=0} = K_b.v_{x=0} \tag{5}$$

Moreover, the analytical solutions of equation (4) can be obtained in term of $v=v(x)$ and the last remains unknown. Therefore, an approximate numerical method is required.

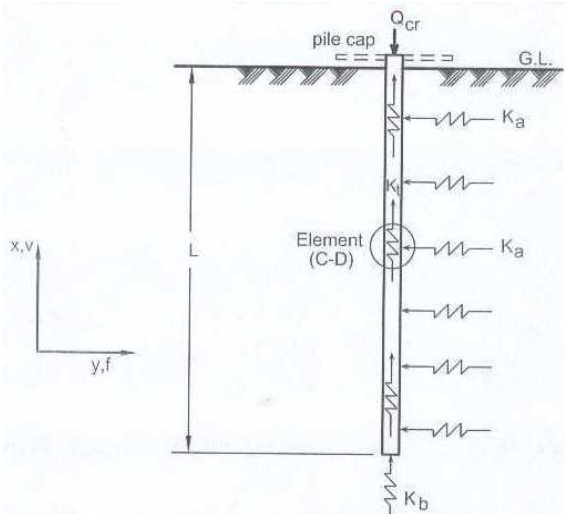

Figure 1: Elastic Micropile in Weak Soil

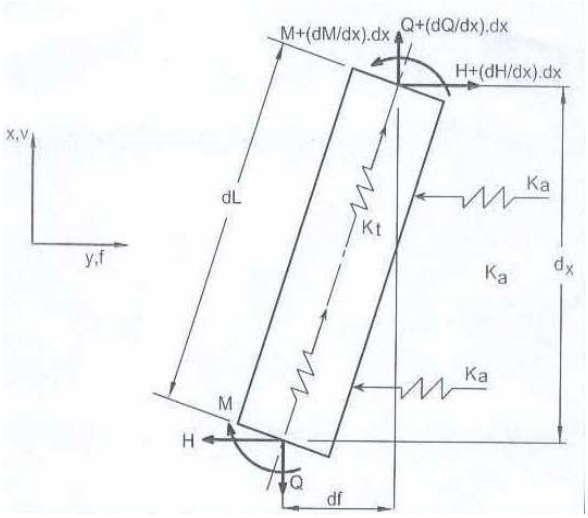

Figure 2: Forces and Moments on Element C-D

Figure 3 shows the adopted central finite-difference of equal spacing (Δx). Where, $\Delta x = L/(N-1)$ and N is the total number of nodes. Then, the differential equation (4) is written in central finite-difference for node (i) as the following:

$$E.A.\frac{v_{i-1} - 2v_i + v_{i+1}}{(\Delta x)^2} - K_{ti}.v_i = 0 \tag{6}$$

To simulate the boundary conditions at the base of micropile (node 1), the forward finite–difference is used as:

$$E.A.\frac{v_2 - v_0}{2\Delta x} = K_b.v_1 \tag{7}$$

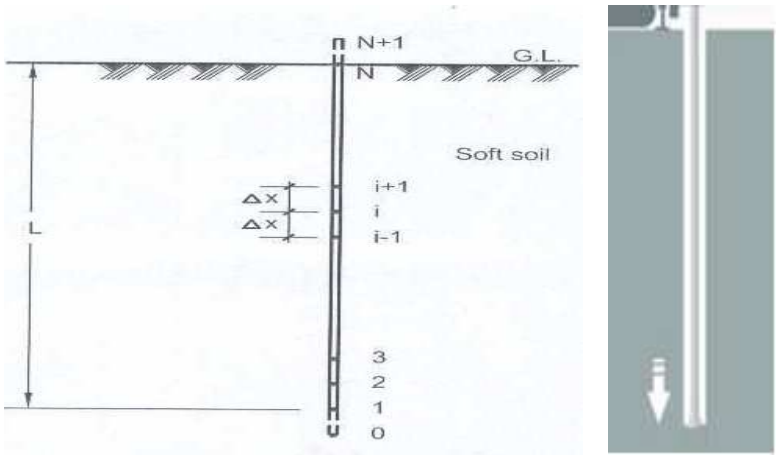

Figure 3: Finite Difference Scheme of Micropile Embedded in Weak Soil

Lateral Direction Equations

Referring to Figure 2, the equilibrium of forces in the horizontal (lateral) direction gives the following equation:

$$\frac{dH}{dx} = K_a.f \tag{8}$$

Moreover, the equilibrium of moments is considered as:

$$dM + Q.df - H.dx = 0 \tag{9}$$

By differentiating equation (9) with respect to *x* and dividing by *dx*, the equation gives the following:

$$\frac{d^2M}{dx^2} + Q.\frac{d^2f}{dx^2} + \frac{dQ}{dx}.\frac{df}{dx} - \frac{dH}{dx} = 0 \tag{10}$$

Hence, the substitution of equation (8) into equation (10), the following equation is given:

$$\frac{d^2M}{dx^2} + Q.\frac{d^2f}{dx^2} + \frac{dQ}{dx}.\frac{df}{dx} - K_a.f = 0 \tag{11}$$

The small–angle bending expression for the moment curvature relationship is:

$$M = -E.I.\frac{d^2f}{dx^2} \tag{12}$$

By substituting equation (12) into equation (11), the governing fourth-order linear differential equation for the lateral direction *f = f.(x)* gives:

$$-E.I.\frac{d^4f}{dx^4} + Q.\frac{d^2f}{dx^2} + \frac{dQ}{dx}.\frac{df}{dx} - K_a.f = 0 \tag{13}$$

Referring to equation (13), it is evident that: (a) equation (13) has no available analytical solution according to the variation of the axial force and (2) by neglecting the skin friction for constant axial force, it reduces to the well-known equation derived by Hetenyi [13] for buckling of beams in the elastic foundation. Therefore, the approximate numerical solution of central finite-difference is used. Hence, the equation (13) is written as:

$$-E.I.\left(\frac{f_{i-2}-4f_{i-1}+6f_i-4f_{i+1}+f_{i+2}}{(\Delta x)^4}\right)+Q.\left(\frac{f_{i-1}-2f_i+f_{i+1}}{(\Delta x)^2}\right)+\left(\frac{-Q_{i-1}+Q_{i+1}}{2.\Delta x}\right).\left(\frac{-f_{i-1}+f_{i+1}}{2.\Delta x}\right)-K_{ai}.f_i=0 \quad (14)$$

By rearranging equation (14), it becomes as:

$$-\left[\frac{E.I}{(\Delta x)^4}\right].f_{i-2}+\left[4\frac{E.I}{(\Delta x)^4}+\frac{Q_i}{(\Delta x)^2}-\left(\frac{-Q_{i-1}+Q_{i+1}}{4(\Delta x)^2}\right)\right].f_{i-1}+\left[-6.\frac{E.I}{(\Delta x)^4}-2.\frac{Q_i}{(\Delta x)^2}-K_{ai}\right].f_i+\left[4.\frac{E.I}{(\Delta x)^4}+\frac{Q_i}{(\Delta x)^2}+\left(\frac{-Q_{i-1}+Q_{i+1}}{4(\Delta x)^2}\right)\right].f_{i+1}-\left[\frac{E.I}{(\Delta x)^4}\right].f_{i+2}=0 \quad (15)$$

Solution Sequence

Equation (15) can be applied for the embedded length of micropile in soft soil, i.e., for nodes *2* to *N-1*. Thus, a set of *N-2* simultaneous homogeneous linear equations in *N+2* unknowns are obtained. So, the matrix form can be given as:

$$\{G\}_{(N-2).(N-2)}.\{f\}_{(N-2)}=0 \quad (16)$$

Where, the coefficients of matrix *{G}* are changed into square matrix by applying the boundary conditions at lower and upper ends of micropile as follows:

- Boundary conditions at the lower end of micropile (node 1).
  - At fixed end: $f_1=0, f_{i-1}=f_{i+1}$ (i.e. deflection=0, slope=0)
  - At Hinged end: $f_1=0, f_{i-1}=f_{i+1}$ (i.e. deflection=0, curvature=0)
  - At free end: $M_1=0, H_1=0$ (i.e. moment=0, horizontal force=0)
- Boundary conditions at the upper end of micropile (node N)
  - At fixed end: $f_N=0, f_{N-1}=f_{N+1}$ (i.e. deflection=0, slope=0)
  - At Hinged end: $f_N=0, f_{N-1}=f_{N+1}$ (i.e. deflection=0, curvature=0)
  - At free end: $M_N=0, H_N=0$ (i.e. moment=0, horizontal force=0)

The initial values for H, Q_{cr} and f_i are required to start the solution. These variables can be estimated by using the results obtained from the linear analysis. In this study, the first iteration gives the linear results by setting all the nonlinear terms equal to zero. After obtaining the solution, the micropile length is modified until reaching the specific accuracy and the curved length of the pile is obtained using a forward numerical integration as:

$$L = \sum_{i=1}^{N-1} \left[1 + \left(\frac{-f_i + f_{i+1}}{\Delta x} \right) \right]^{0.5} .\Delta x \qquad (17)$$

The computed length of pile obtained from equation (17) is compared with the actual length. If the difference between the computed length and the actual length is more than 1%, the procedure is repeated to reach the required accuracy. Hence, finite-difference scheme for micropile, as shown in Figure 3, was simulated using MATLAB-SIMULINK programming language under MATLAB package of version 7.14. Where, the simulation was based on MATLAB-SIMULINK toolboxes which are suitable for differential equations. Fixed step integration algorithm of 0.1 ms based on Euler method has been used to solve the system.

NUMERICAL APPLICATION

The theoretical approach is applied on a hollow pipe micropile of outer diameter of 20.5 cm and inner diameter of 19.6 cm. So, the micropile has: (a) cross section area of pile (A)=28.33 cm^2, (b) moment of inertia (I) =2848.7 cm^4, and (c) elasticity modulus (E) =200 x 10^6 kN/m^2. In this study, the micropile is fully embedded in soft soil and it is analyzed for the followings:

- Moduli of surrounding soil subgrade reactions were considered, 500kN/m^3, 1000kN/m^3, 5000kN/m^3 and 10000kN/m^3.
- Three micropile-end conditions were considered, free, hinge and fixed end.
- The micropile length is considered to be a long pile or a flexible pile and its behavior is similar to that of semi-infinite pile.

The effect of the studied variables on the buckling behavior of micropile are presented in dimensionless form, as shown in Figures 5-11, showing the relationships between the critical load ratio, R ($R=Q_{cr.1}/Q_{cr.2}$), against the lateral deflection ratio, F ($F=f_{max.}/L$). Where, $Q_{cr.1}$ is the critical load obtained from the small-angle bending analysis, $Q_{cr.2}$ is the critical load obtained from the linear analysis (i.e. all nonlinear parameters equal zero), f_{max} is the maximum lateral deflection of micropile and L is the length of micropile.

From the analysis of the studied factors affecting the buckling behavior of micropile, it is evident that these factors have a significant effect on the critical buckling load ratio (R). Also, it is clear that: (a) the critical buckling loads computed from small-angle bending analysis ($Q_{cr.1}$) are equal and approximately in close to those obtained by linear analysis ($Q_{cr.2}$) at low values of lateral buckling; and (b) with the increase of the given lateral buckling, the values of $Q_{cr.1}$ increase gradually compared to $Q_{cr.2}$, (R>1.0).

According to results of analysis and the relationships between the critical buckling load ratio (R) and the lateral deflection ratio (F), as plotted in Figures 5-11, the controlling factors affecting the buckling of micropile can be described as the followings:

Subgrade Reactions

Figure 4 shows the lateral deflection profiles of micropiles hinged-hinged, fixed- hinged and fixed-fixed end conditions. Micropiles are fully embedded in soils of three different values of normal subgrade reaction (K_a). The effect of normal subgrade reaction modulus (K_a) on the lateral deflection is considered. The deflection profiles show that:

- The deflection values are influenced by the value of K_a. Where, with the increase of K_a values the lateral resistance to the lateral deflection increases. Hence, the lateral deflection is restricted and decreased.
- The end conditions of micropile play a considerable effect on lateral deflection. As the increase of fixation, the lateral deflection decreases.

On the other hand, Figures 5-7 show the relationships between the critical buckling load ratio (R) and the given lateral deflection ratio (F) at the variation values of K_a, K_t and K_b. Based on the results analysis:

- As the values of K_a increase, the values of the buckling load ratio (R) increase regardless to values of L, K_t and K_b. For instant, at the lateral buckling ratio (F)= 10% and 20%, the buckling load ratio increases by about 2% and 15% respectively for the maximum considered value of K_a (10000 kN/m^3). While, at low value of K_a (500 kN/m^3), the increase of R is about 3% at F=20%, as shown in Figure 5.
- The values of R decrease slightly with the increase of K_t regardless to values of L, K_a and K_b. For example, at F=20%, the value of R increases by about 4% for K_t =500kN/m^3 and by about 3.25% for K_t =10000kN/m^3, as plotted in Figure 6.
- The values of R increase slightly with the increases of K_b values regardless values of L, K_a and K_t. The value of R increases by about 4% for K_b=500kN/m^3 and by 5% for K_b=10000kN/m^3 at F=20%, see Figure 7.

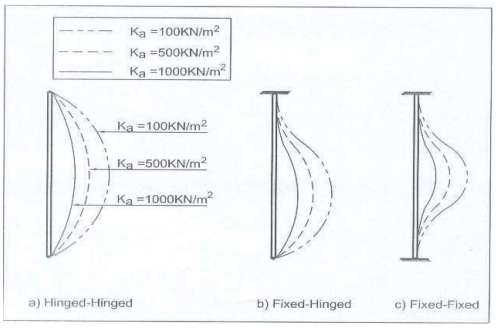

Figure 4: Profile of $f_{max.}$ at Various K_a

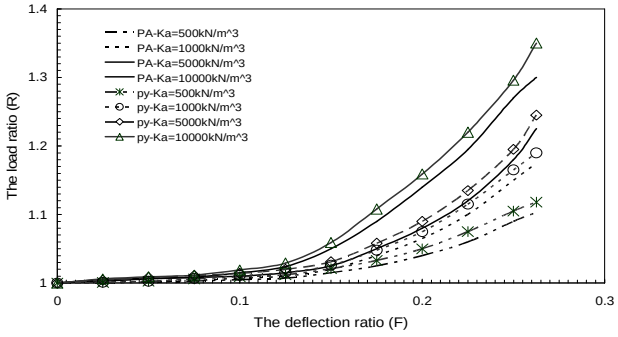

Figure 5: Relation between R and F at Various K_a (L=20m, K_b=1000kN/m^3 and $_t$=1000kN/m^3)

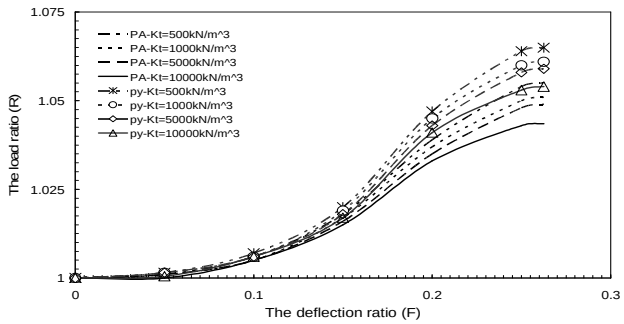

Figure 6: Relation between R and F at Various K_t (L=20m, K_a=1000kN/m^{3}and K_b=1000kN/m^3)

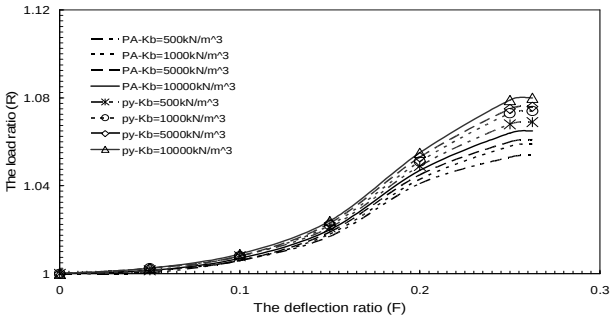

Figure 7: Relation between R and F at Various K_b (L=20m, K_a=1000kN/m^{3}and K_t=1000kN/m^3)

Boundary Conditions

The boundary conditions have a significant effect on the buckling load of micropile with the increase of the given lateral buckling. It was observed that with the increase of K_a value the lower end will be similar to the fixed end regardless the type of the boundary conditions. According to the analysis results the variations of boundary conditions, it is clear that:

- Micropile buckling load is influenced and controlled by the upper end conditions. The increase in the buckling load ratio (*R*) with the lateral deflection ratio (*F*) will be similar for piles having the same upper end condition.
- The changes in the buckling load ratio (*R*) with the given ratio *F* for micropile hinged at its upper end is approximately the same changes for micropiles fixed and free upper ends, as indicated in Figures 8-10. On the other hand, for a micropile free at its base, the increase in *R* is less than that for a lower hinged or fixed ends except at very high values of normal modulus of subgrade reaction (K_a). For example, at *F*=20%, the increase of the ratio *R* is about 10% for piles with hinged and fixed lower end. While, *R* value increases by about 6% for micropile free lower end, Figure 8.

Micropile Length

The relationship between the critical buckling load ratio (*R*) and the lateral deflection ratio (*F*) due to the variation of micropile length (*L*) are shown in Figure 11. The results indicated that the micropile length (*L*) has a significant effect on the values of both *R* with *F* and related to the changes of micropile buckling load with pile length (*L*). Also, it is observed that:

- For large length of micropile, the increase in the ratio *R* with the ratio *F* is less than that for small length. For instant, at *F*=20%, the increase of *R* is about 5% and 10% for *L*=25m and 10m respectively.
- The value of *R* trend increases with the increase of *L*. For example, the values of *R* increase by 1.5% and 5% at *F*=10% and 20% respectively for *L*=25m, while, that values increase by 2.5% and 10% for *L*=10m.

COMPARISON

The lateral load-displacement (p-y) method was used for comparison because the p-y method is capable to: (1) represent wide range of soil and loading conditions in realistic manner; and (2) be in reasonable agreement with the field loading results. Also, this method has been chosen to validate the proposed method. The p-y analysis was performed using the computer program GeoFEAP with internally generated p-y curves according to the criteria of Resse [14]. The soil parameters required to develop the p-y analysis for the studied cases are given in Table 1.

Table 1: Soil Parameters of the Soil Used in p-y Analysis

Properties	Quantity	Properties	Quantity
Wet unit weight (γ_{wet})	17.0 kN/m^3	Young's modulus (E_s)	2.5 Mpa
Cohesion (c)	10.0 kN/m^2	Poisson's ratio (μ)	0.40
Internal friction angle (ϕ)	7.5 degree	Rankine earth pressure coefficient	1.3
Permeability coefficient	1x10^{-5} cm/sec.	Interface reduction factor	1.0

Comparisons between the present analysis (PA) and p-y method for the lateral deflection (buckling) of the micropile are shown in Figures 5-11. Referring to the analysis and comparison, it is evident the followings:

- The two methods (PA & p-y) produce almost identical solutions of micropile buckling load ratio (R) against its lateral deflection ratio (F).
- The two methods are approximately in close agreement at the deflection ratio (F) ≤ 15%. The discrepancy between the two methods will increase as the deflection ratio increases. The overall agreement of the two methods is quite acceptable.
- The maximum variation in predicting the critical buckling ratio (R) obtained from the p-y method is about 15% more than that of the proposed method in case of lateral deflection ratio (F) > 15%.
- The capability of the proposed technique makes it more useful in practice to provide the buckling behavior of micropile fully embedded in weak soils.

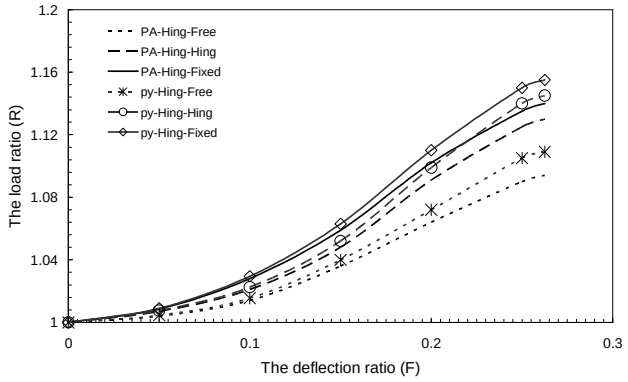

Figure 8: Relation between R and F at Various Lower End Conditions for Hinged Upper End (L=20m, K_a=1000kN/m3, K_b=1000kN/m^3 and K_t=1000kN/m^3)

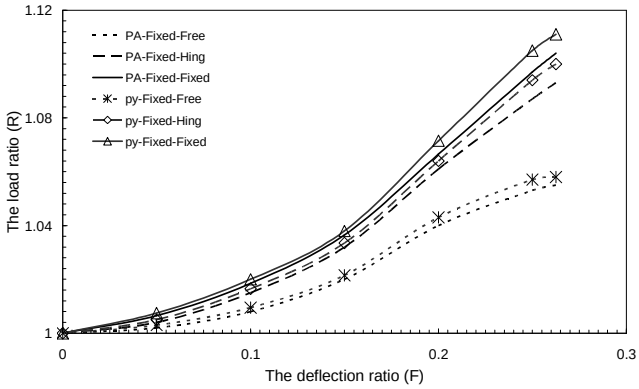

Figure 9: Relation between R and F at Various Lower End Conditions for Fixed Upper End, (L=20m, K_a=1000kN/m3, K_b=1000kN/m^3 and K_t=1000kN/m^3)

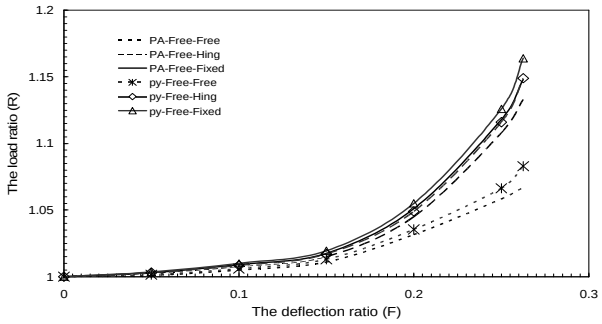

Figure 10: Relation between R and F at Various Lower End Conditions for Free Upper End K_b=1000kN/m^3 and K_t=1000kN/m^3)

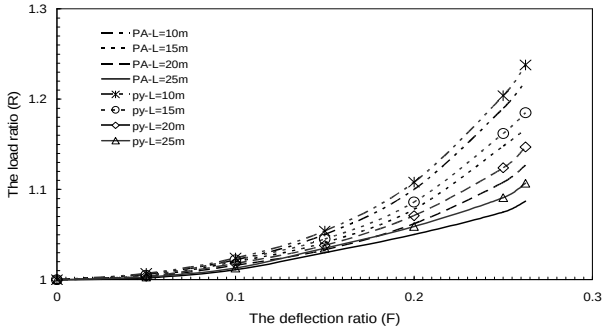

Figure 11: Relation between R and F at Various Micropile Length, (K_a=1000kN/m3, K_b=1000kN/m^{3}and K_t=1000kN/m^3)

CONCLUSIONS

The effect of subgrade reactions, pile end conditions and pile length on the critical buckling load of micropile was analyzed. Based on the analysis results, the following conclusions could be drawn:

- The critical buckling load computed from small-angle bending analysis ($Q_{cr.1}$) is approximately in close to those obtained by linear analysis ($Q_{cr.2}$) at low values of lateral buckling (F<15%).

- The values and variations of the soil subgrade reactions affect the axial buckling load and the lateral deflection of micropile. The critical buckling load ratio (R) increases with the increase of K_a and K_b. But, R value decreases with the increases of K_t.
- The critical buckling loads are controlled by the upper end condition. The changes in the buckling load ratio (R) for hinged upper end pile are approximately similar to that for fixed and free upper end piles. While, for free lower end pile, the increase of R is less than that for hinged or fixed lower ends.
- With the increase of micropile length, the critical buckling load ratio(R) decreases and vice versa.
- Comparison with documented p-y method confirms that the proposed method provides reliable analysis for critical buckling load of micropile embedded in a homogeneous soft soil layer.
- From the aforementioned conclusions, it is recommended that the analysis is required for each specific case to estimate the micropile buckling load. Therefore, more theoretical analysis and experimental works are necessary to assess the behavior of micropile at variant cases.

REFERENCES

1. Veludo, J., Julio, E.N.B.S. and Costa, D.D., "Compressive strength of micropile-to-grout connections", Construction and Building Materials Magazine, Vol. 26, No. 1, pp. 172-179, 2012.
2. Daniel, D., Uranowski, P.E. Scott, D. and Scott, S.P.E., "Micropiles in Karstic Dolomite Similarities and Differences of Two Case Histories", Civil Engineering Journal, ASCE, Vol. 73, No. 1, pp. 14-81, 2004.
3. Tarek, M.F., "A Study on the Group Behavior of Micropiles", 9th International Colloquium on Structural and geotechnical Engineering, Ain-Shim University, Faculty of Engineering, Cairo, Egypt, pp. 1-13, 2001.
4. Northwestern University, "Evaluation of compaction Grouted minipiles", The Northwestern University, National geotechnical Experimentation Site, USA, pp. 1-26, 1998.
5. El-Kasaby, E.AA., "Using Micropiles for Restoration and Strengthening Egyptian Archaeological Buildings", 5th International Conference on Deep Foundation Practice, Singrapore, pp. 191-199, 2001.
6. Abou-Rayan, A.M., "Finite Element Simulation of Laterally Loaded Single Pile", Engineering Research Journal, Helwan University, Vol. 93, pp. 83-98, 2004.
7. Ashour, M., and Norris, G., "Lateral Loaded Piles Response in Liquefied Soil", Journal of Geotechnical and Geoenviromental Engineering, ASCE, Vol. 129, pp. 404-414, 2003.
8. Zanuy, C., Fuente, P. and Pinilla, M., “Bending strength of threaded connections for micropiles”, Journal of constructional Steel Research, Vol. 78, pp. 68-78, 2012
9. Sun, S.W., Zhu, B.Z. and Wang, J.C., "Design method for stabilization of earth slopes with micropiles", Soil and Foundations, Vol. 53, No. 4, pp. 487-497, 2013.
10. Ansari, K.A., "Large–Angle Bending Analysis for Buckling of slender columns", Computers and Structures, Vol. 137, pp. 357-363, 2003.

11. Polous, H.G., "The Influence of Shaft Length on Pile Load Capacity in Clays", Geotechnique 52, pp. 145-152, 2002.
12. Tsukada, Y., Miura, K., Tsubokawa, Y., Otani, Y., You, G.L. and Ishito, M., "Mechanism of bearing capacity of surface footings reinforced with micropiles", Journal of Geotechnical and Geoenvironmental Engineering, ASCE, Vol. 129, No. 9, pp.794-803, 2003
13. Leroueil, S., Roy, M., and Marted, G., "Evaluation of Shaft Friction in Sensitive Clays from Piezocone Tests", 14th International conference of Soil Mechanics and foundation Engineering, Hamburg, Vol. 1, pp. 147-150, 1997.
14. Orlando, L., "Detecting steel rods and micro-piles: A case history in a civil engineering application", Journal of applied geophysics, Vol. 81, pp. 130-138, 2012.